**Supporting Information**

# A "Special" Solvent to Prepare Alloyed $Pd_2Ni_1$ Nanoclusters on a MWCNT Catalyst for Enhanced Electrocatalytic Oxidation of Formic Acid

**Pingping Yang [1,2,†], Li Zhang [1,2,†], Xuejiao Wei [1], Shiming Dong [1], Wenting Cao [1], Dong Ma [1], Yuejun Ouyang [1],**
**Yixi Xie [2,*], and Junjie Fei [2,*]**

[1] College of Chemistry and Materials Engineering, Huaihua University; Huaihua, 418008, Hunan, China yangpingping0218@163.com (P.Y.); zhanglicsu2013@163.com (L.Z.); wei1348137@163.com (X.W.); dsm20032022@163.com (S.D.); cwt1822707678@163.com (W.C.); md12341110@163.com (D.M.); oyyj0816@163.com (Y.O.)
[2] College of Chemistry, Xiangtan University, Xiangtan 411105, Hunan, China
* Correspondence: xieyixige@xtu.edu.cn (Y.X.); fei_junjie@xtu.edu.cn (J.F.)
† These authors contributed equally to the work.

## Table of Contents:

### 1. Calculate details

The calculation details are as follows:

"To calculate the average particle size of the alloy, we used ImageJ software to calculate. Firstly, select a TEM image with enough sample size of 100 nm scale bar, enlarge the TEM image to a size that is conducive to measuring the particle size, draw a straight line on the scale bar using the line measurement tool, and calibrate the line to the length of 100 nm of the scale bar; then use the linear measurement tool to randomly measure the particle size of 200 samples in the image; finally, calculate the average particle size of 200 samples. Here we have also added part of the original text: To measure the particle size of the alloy, 200 random samples were chosen from the TEM images." (Paragraph 1 of support information part)

The average size of the alloy particles was calculated to be 3.6 nm ($Pd_2Ni_1$/CNTs) and 4.1 nm (Pd/CNTs).

### 2. Supplementary Figures

**Figure S1**. The corresponding particle size distribution of Pd/CNTs.

**Figure S2**. TEM and HRTEM images of Pd/CNTs.

**Figure S3**. EDX line-profiles (a), spot scanning (b) of $Pd_2Ni_1$ nanoparticle (where Pd is in red and Ni in blue) of $Pd_2Ni_1$/CNTs.

**Figure S4**. TEM images and size distribution histograms of $Pd_2Ni_1$/CNTs (A, B) and Pd/CNTs (C, D) after the current-time measurements in 1.0 M HCOOH + 0.5 M $H_2SO_4$ solution.

## 3. Supplementary Tables

**Table S1.** Elemental composition of the samples obtained from ICP.

**Table S2** A recent literatures survey of the activity of FAOR electrocatalysts.

**Table S3.** Pd 3d peaks of $Pd_2Ni_1$/CNTs and Pd/CNTs.

## 4. Supplementary References

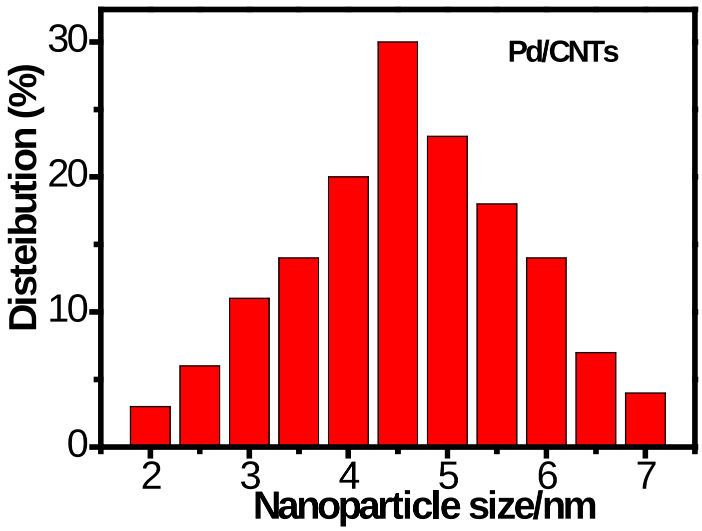


**Figure S1**. The corresponding particle size distribution of Pd/CNTs.

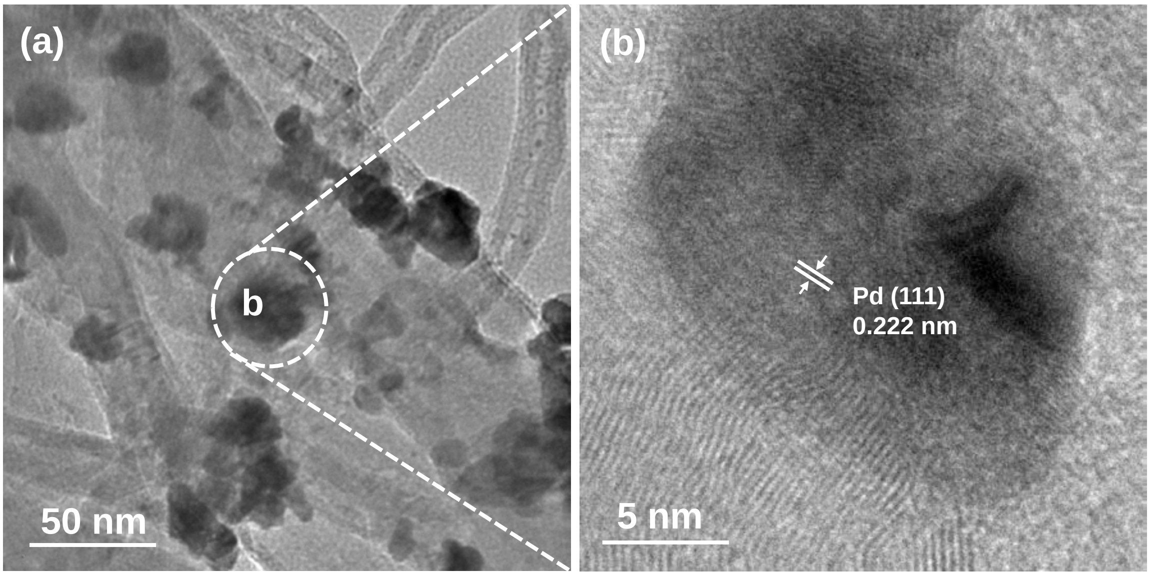


**Figure S2**. TEM (a) and HRTEM (b) images of Pd/CNTs catalyst.

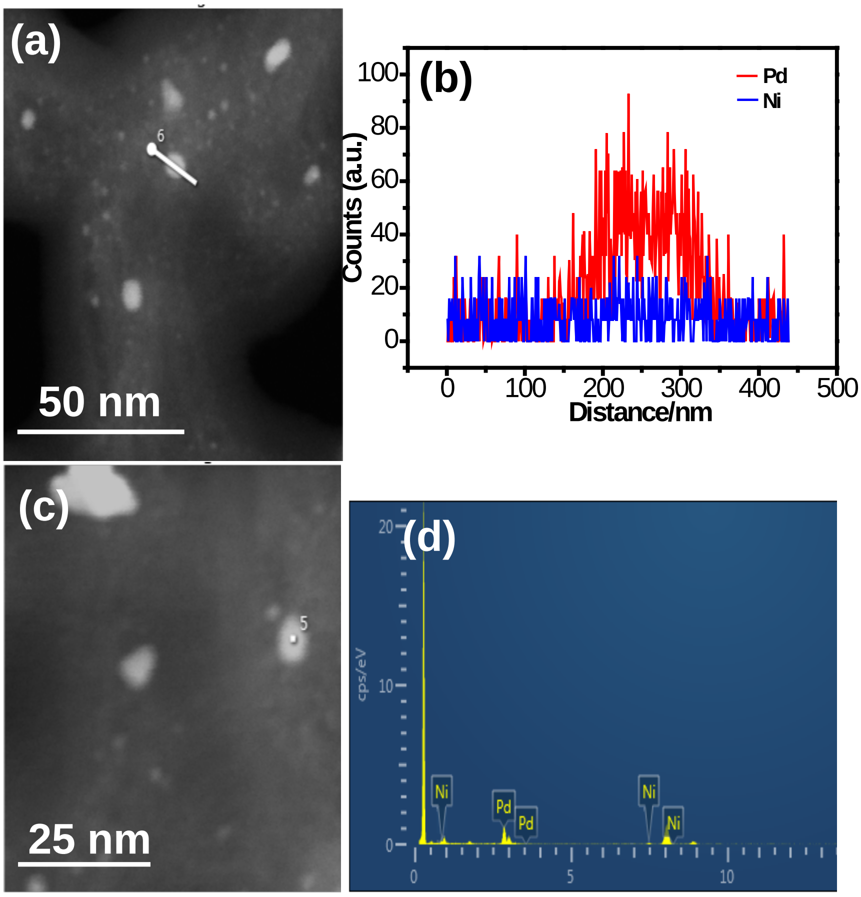


**Figure S3**. EDX line-profiles (a, b), spot scanning (c, d) of a $Pd_2Ni_1$ nanocluster (where Pd is in red and Ni in blue).

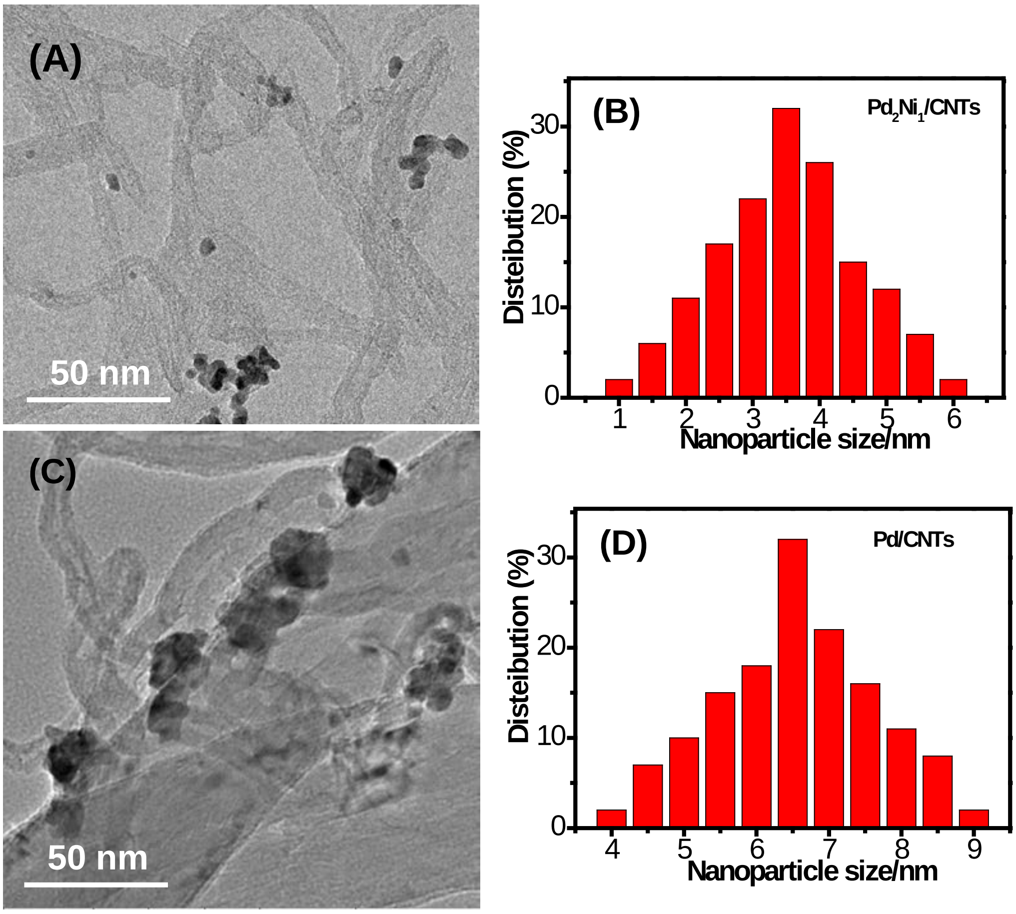


**Figure S4** TEM images and size distribution histograms of $Pd_2Ni_1$/CNTs (A, B) and Pd/CNTs (C, D) after the current-time measurements in 1.0 M HCOOH + 0.5 M $H_2SO_4$ solution.

**Table S1.** Pd 3d peaks of $Pd_2Ni_1$/CNTs and Pd/CNTs.

| **Catalysts** | **$Pd^0$ $3d_{5/2}$ (eV)** | **$Pd^0$ $3d_{3/2}$ (eV)** | **$Pd^{2+}$ $3d_{5/2}$ (eV)** | **$Pd^{2+}$ $3d_{3/2}$ (eV)** |
|---|---|---|---|---|
| $Pd_2Ni_1$/CNTs | 335.6 | 340.8 | 336.0 | 341.5 |
| Pd/CNTs | 335.8 | 336.6 | 341.2 | 341.6 |

**Table S2** a recent literatures survey of the activity of FAOR electrocatalysts.

| Catalysts | Mass activity ($mA\ mg^{-1}{}_{Pd}$) | References |
|---|---|---|
| **$Pd_2Ni_1$/CNTs** | **3351.6** | **This work** |
| PdCo nanodots | 1362.1 | [1] |
| PdCu nanochains | 1108.2 | [2] |
| PdCu clusters | 1289.0 | [3] |
| coral-like PdCu | 1050.0 | [4] |
| $Pd_6Co$ nanocrystals | 430.8 | [5] |
| PdCu nanoparticles | 194.5 | [6] |
| (3D) porous PdSn | 553.4 | [7] |
| PdCu porous network | 517.0 | [8] |
| PdeFe nanoparticles | 1000.0 | [9] |
| PdCu/CNTs | 252.0 | [10] |

**Table S3.** Elemental composition of the samples obtained from ICP.

| Elements / Catalysts | Pd(wt.%) | Ni(wt.%) | Atomic ratios |
|---|---|---|---|
| $Pd_2Ni_1$/CNTs | 18.6 | 9.31 | 2:1 |
| $Pd_1Ni_1$/CNTs | 19.2 | 17.8 | 1:1 |
| $Pd_1Ni_2$/CNTs | 19.6 | 38.1 | 1:2 |
| Pd/CNTs | 16.3 | - | - |

# References


[1] Zhang. L-Y, et al. Palladium-cobalt nanodots anchored on graphene: In-situ synthesis, and application as an anode catalyst for direct formic acid fuel cells. Appl Surf Sci 2019, 469, 305-311.

[2] Zhang. L-Y, et al. Twisted palladium-copper nanochains toward efficient electrocatalytic oxidation of formic acid. J Colloid Interf Sci 2019, 537, 366-374.

[3] Zhang. Z, et al. Facile fabrication of stable PdCu clusters uniformly decorated on graphene as an efficient electrocatalyst for formic acid oxidation. Int J Hydrog Energ 2019, 44, 2731-2740.

[4] Zheng J, et al. Coral-like PdCu Alloy Nanoparticles Act as Stable Electrocatalysts for Highly Efficient Formic Acid Oxidation. ACS Sustain Chem Eng 2019, 7, 15354-15360.

[5] Zhang. L-Y, et al. Facile one-pot surfactant-free synthesis of uniform $Pd_6Co$ nanocrystals on 3D graphene as an efficient electrocatalyst toward formic acid oxidation. Nanoscale 2016, 8, 1905-1909.

[6] Wang. L, et al. Pd-Cu/C electrocatalysts synthesized by one-pot polyol reduction toward formic acid oxidation: Structural characterization and electrocatalytic performance. Inter J Hydrog Energ. 2015, 40, 1726-34.

[7] Sun. D-D, et al. Nanobranched porous palladium-tin intermetallics: One-step synthesis and their superior electrocatalysis towards formic acid oxidation. J Power Sources 2015, 280, 141-146.

[8] Yang. F, et al. Pd-Cu alloy with hierarchical network structure as enhanced electrocatalysts for formic acid oxidation. Inter J Hydrog Energ 2016, 41, 6773-6780.

[9] Feng. A-N, et al. Surfactant-free Pd-Fe nanoparticles supported on reduced graphene oxide as nanocatalyst for formic acid oxidation. Inter J Hydrog Energ 2017, 42, 15196-15202.

[10] Zhu. F-C, et al. High activity of carbon nanotubes supported binary and ternary Pd-based catalysts for methanol, ethanol and formic acid electro-oxidation. J Power Sources 2013, 242, 610-20.